Inorganic Chemistry Communications 159 (2024) 111709

Contents lists available at ScienceDirect

Inorganic Chemistry Communications

journal homepage: www.elsevier.com/locate/inoche

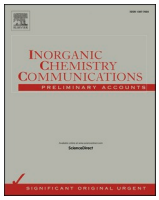

Pharmaceutical investigation of 2-Amino-4-(2-fluorophenyl)-5,10-dioxo-5,10-dihydro-4*H*-benzo[*g*] chromene-3-carbonitrile via computational studies

N. Thirughanasambantham [a], V. Balachandran [a,*], B. Narayana [b,d], C. Sivakumar [a], A. Jayashree [b], M. Kavimani [c]

[a] Department of Physics, Arignar Anna Government Arts College (Affiliated to Bharathidasan University), Musiri, Tiruchirappalli 621211, India
[b] Department of Studies in Chemistry, Mangalore University, Mangalagangotri 574 199, India
[c] Department of Physics, Cauvery College for Women (Autonomous), Tiruchirappalli 620 018, India
[d] K K University, Bihar Sherif, Berauti, Bihar 803115, India

ARTICLE INFO

Keywords:
DFT
Chromene
Carbonitrile
Vibrational Analysis
Molecular Docking

ABSTRACT

The atomistic and spectroscopic data of 2-Amino-4-(2-fluorophenyl)-5,10-dioxo-5,10-dihydro-4*H*-benzo[*g*] chromene-3-carbonitrilehad beengained from DFT/B3LYP 6-31G(d,p) and 6–311++G(d,p) basis set enumerations. Themolecular geometrywasfullyoptimized, vibrational spectra were logged and potential energy distribution (PED) was allocated based onnormal modes of vibrations. Besides, the molecular electrostatic potential (MEP), HOMO-LUMO, and Mulliken charges wereimplemented. The biotic outcomewas prophesied with the help of molecular docking results.

1. Introduction

Carbonitrile with 4*H*-Chromene derivatives wasascertained in natural compounds and explained pharmacological and biotic activities[1]. The compound 2-amino-4-(2-fluorophenyl)-5, 10-dihydro-4H-benzo[g] chromene-3-carbonitrile (AFBCC) derivative is known to have antitubercular and anti-fungal activity. Aromatic nitrile possesses versatile utilities and is indispensable not only in organic synthesis but also in the chemical industry.The amino derivatives have been used to acquire new supramolecular electrolytes which are exploited in dye-sensitized solar cells[2]. 4*H*-Chromene derivatives are crucial arena in organic and medicinal chemistry. It exists in a class of naturally ensued benzopyran derivatives are expansive in biological applications, it contains antiproliferative[3], anticancer[4], antibacterial[5], antiviral[6],and potent apoptosis inducers[7]. Chromene derivatives have multiple biological activities in organic synthesis and medicinal studies for further progress [8]. The quantum chemical calculations and vibrational spectra forthe AFBCC compound have not been reported as yet. AFBCC compound has structural and physiochemical properties and was exposed usingDensity Functional Theory (DFT). The affinity between these properties and the biotic activity of the AFBCC compound is used to manifest[9]. At present work, the geometrical parameters, and vibrational wavenumbers are reckoned using the B3LYP/6-31G (d, p) and B3LYP/6–311++G (d, p) basis sets. Many properties like frontier molecular orbitals (FMO)various chemical descriptors, and molecular electrostatic potential analysis are executed to provide information about charge transfer in the internal molecule. Benzo[g]chromene spectacle an assortment of biological activities, it encompasses anticancer, antifungal, Ubiquinol-cytochrome-c reductase inhibitor, and cytochrome P450 activities with the help of pass online[10]. Molecular docking studies are also reported to establish its biological activity.

2. Experimental studies

The Fourier Transform Infrared (FT-IR) spectrum was recorded for the AFBCCcompound at the range of 4000–400 $cm^{-1}$and was effectuated with a Perkin-Elmer spectrometerin the KBr pellet technique. The resolutionof the spectral is 0.1 cm^{-1}. The Fourier Transform Raman (FT-Raman) spectrum was recorded in the Bruker RFS 27 MultiRAM standalone FT-Raman spectrometer in the frequency range 4000–0 cm^{-1}. The spectral measurements are effectuated in the source of laser is Nd: YAG was operating at 1064 nm with 200 mW power.

* Corresponding author.
E-mail address: brsbala@rediffmail.com (V. Balachandran).

https://doi.org/10.1016/j.inoche.2023.111709
Received 13 August 2023; Received in revised form 21 October 2023; Accepted 7 November 2023
Available online 9 November 2023

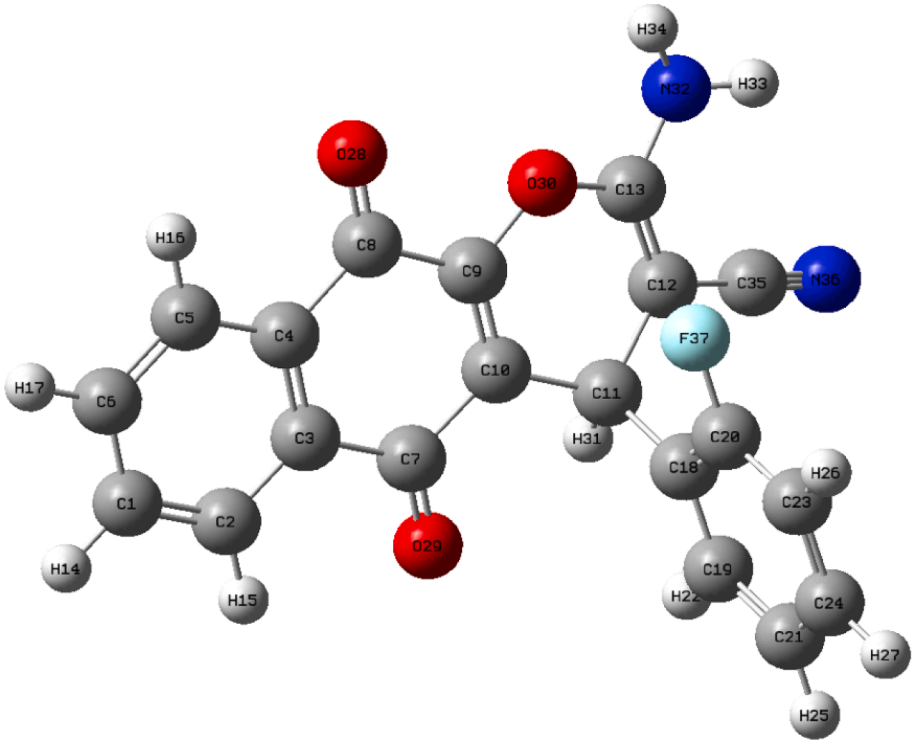

Fig. 1. Optimized molecular structure of AFBCC compound.

3. Computational studies

The computational studies of AFBCCwereaccomplishedin Becke, 3-parameter, Lee-Yang-Parr [111213]at the basis set B3LYP/6-31G (d, p) and 6–311++G (d, p) by the Gaussian 09 W[14] software package. It helps to compute the vibrational assignments, geometrical parameters, frontier molecular orbital, molecular electrostatic potential (MEP), and Mulliken atomic charges. The normal modes wereallocated according to the potential energy distributions (PEDs) using theVibrational Energy Distribution Analysis (VEDA) program and viewable of the Gauss View 6.0 program. The molecular docking studies were executed by Auto dock tool version 1.5.6 software and the outcomes are pictorial in Pymol software and Discovery Studio software.

4. Result and deliberation

4.1. 4.1.Optimized parameter

The optimized molecular structure of AFBCC which accompanies the enumeration of atoms is exhibited in Fig. 1. Geometrical parametersare reckoned by DFT/B3LYP 6-31G (d, p) and DFT/B3LYP 6–311++G (d, p) which were associated with XRD data[15]. The reckoned geometrical parameter is correlated with the crystal data of 2-Amino-4-(2-chlorophenyl)-5,10-dioxo-5,10-dihydro-4H-benzo[g]chromene-3-carbonitrile[16]. Typically, the bond lengths are parallel with the experimental value. In this, all the bond lengths are almost equal except the fluorine atom in the plane benzene ring, it is due to the swap of the fluorine and carbonitrile in the plane of anthrance[15]. According to the experimental valueof the optimized bond length of six contrasting C–C lengths are C2-C3 < C7-C10 < C4-C8 < C10-C11 < C11-C18 (1.380——1.5240) Å is correlated to computed value C2-C3 < C7-C10 < C4-C8 < C10-C11 < C11-C18 (1.397——1.530) Å. The theoretical values of C20-F37, C13-C32, and N32-H33 are 1.350 Å, 1.470 Å, and 1.000 Å higher than the experimental values which are correlated to 1.300 Å, 1.334 Å, and 0.860 Å. The bond angle is formed between three atoms across at least two covalent bonds. Concurrently, the bond angle also slightly deviated from the XRD data[17].

C12-C13-N32 = 127.02 Å (Cal.) < C12-C13-N32 = 127.80 Å (Exp.).

C10-C9-O30 = 123.44 Å (Cal.) < C10-C9-O30 = 124.60 Å (Exp.).

The bond angles are excellent with experimental values that are proclaimed in Table 1.

4.2. Vibrational analysis

Vibrational spectroscopy is an energy-sensitive approach based on the periodic change in dipole moment (IR) or polarizabilities (Raman) generated by molecule or atom vibrations. The vibrational assignments are reckoned in the basis sets of DFT/B3LYP/ 6-31G (d, p) and 6–311++G (d, p). The IR intensities and Raman intensities are inclusive of characteristic group frequencies[18]. In AFBCC dwell 37 atoms and 105 vibrations which are split as 37 stretching, and 34modes each out-of-plane and in-plane bending vibration. The observed and reckoned DFT/B3LYP/6-31G (d, p) and DFT/B3LYP/ 6–311++G (d, p) spectra were exhibited in Figs. 2 and 3. The vibrational assignments of fundamental modes of AFBCC inclusive of observed and computed frequencies have been proclaimed in Table 2. AFBCC encompasses six functional groupsCarbon-Carbon, Carbon-Hydrogen, Carbonyl, Carbon-fluorine, Carbonitrile, and Aminovibrations are proclaimed following.

4.2.1. AminoVibrations

The AFBCC molecule is a genre of the NH_2 group itencompasses carbonitrile and fluorophenyl. The NH_2molecule anticipates one symmetric, one asymmetric, one scissoring, and one rocking N–H stretching vibration. The NH_2 asymmetric stretching exceeds the symmetric stretching. In N–H, stretching frequency occurs in the rangeof 3500–3200 cm^{-1},Muhammed Hanif et al[19]. In the present case, N–H symmetric and asymmetric stretching vibration was observed in3252 and3320cm^{-1},and the same wavenumber observed in the FT-IR spectrum is 3319 cm^{-1} in asymmetric and 3250 cm^{-1} in symmetric. The NH_2 scissoring mode is granted in the region 1650–1590 cm^{-1}, Ahmet Atac et al[20]. In the title molecule, the NH_2 scissoring mode is computed at 1611 cm^{-1} in B3LYP/6–311++G (d, p). Rocking mode is

Table 1
Optimized molecular geometry parameter of 2-Amino-4-(2-fluorophenyl)-5,10-dioxo-5,10-dihydro-4*H*-benzo[*g*]chromene-3-carbonitrile.

Bond length	B3LYP/ 6-31G (d,p) Å	B3LYP/ 6–311++G (d,p) Å	XRD* Å	Bond angle	B3LYP/ 6-31G (d,p) (°)	B3LYP/ 6–311++G (d,p) (°)	XRD* (°)
C1-C2	1.39	1.37	1.38	C2-C1-C6	120.24	120.45	120.00
C1-C6	1.40	1.43	1.38	C2-C1-H14	119.81	120.96	120.00
C1-H14	1.09	1.10	0.93	C6-C1-H14	119.95	118.59	120.00
C2-C3	1.40	1.43	1.38	C1-C2-C3	119.97	120.76	120.20
C2-H15	1.09	1.10	0.93	C1-C2-H15	121.61	121.16	119.90
C3-C4	1.41	1.43	1.40	C3-C2-H15	118.42	118.08	119.90
C3-C7	1.49	1.40	1.49	C2-C3-C4	119.76	118.79	119.70
C4-C5	1.40	1.43	1.39	C2-C3-C7	119.43	121.70	119.80
C4-C8	1.49	1.40	1.48	C4-C3-C7	120.82	119.51	120.60
C5-C6	1.39	1.37	1.37	C3-C4-C5	120.03	118.79	119.60
C5-H16	1.09	1.10	0.93	C3-C4-C8	120.69	119.51	120.20
C6-H17	1.09	1.10	0.93	C5-C4-C8	119.28	121.70	120.20
C7-C10	1.48	1.40	1.47	C4-C5-C6	119.88	120.77	120.00
C7-O29	1.23	1.43	1.22	C4-C5-H16	118.54	118.08	120.00
C8-C9	1.50	1.40	1.49	C6-C5-H16	121.59	121.16	120.00
C8-O28	1.22	1.43	1.22	C1-C6-C5	120.13	120.45	120.50
C9-C10	1.35	1.43	1.34	C1-C6-H17	120.00	118.56	119.70
C9-O30	1.36	1.43	1.37	C5-C6-H17	119.87	120.99	119.70
C10-C11	1.51	1.43	1.51	C3-C7-C10	118.13	120.98	118.60
C11-C12	1.52	1.37	1.52	C3-C7-O29	121.51	119.50	121.80
C11-C18	1.53	1.54	1.52	C10-C7-O29	120.37	119.53	119.60
C11-H31	1.10	1.07	0.93	C4-C8-C9	116.09	120.98	116.80
C12-C13	1.36	1.43	1.34	C4-C8-O28	123.12	119.50	122.60
C12-C35	1.42	1.54	1.42	C9-C8-O28	120.79	119.53	120.70
C13-O30	1.37	1.37	1.38	C8-C9-C10	124.17	119.51	123.50
C13-N32	1.36	1.47	1.33	C8-C9-O30	112.39	121.70	111.90
C18-C19	1.40	1.40	1.39	C10-C9-O30	123.44	118.79	124.60
C18-C20	1.40	1.40	1.38	C7-C10-C9	119.97	119.51	120.30
C19-C21	1.40	1.40	1.38	C7-C10-C11	118.36	121.70	117.80
C19-H22	1.09	1.10	0.93	C9-C10-C11	121.66	118.78	121.80
C20-C23	1.39	1.40	1.39	C1-C11-C12	108.67	120.77	108.40
C20-F37	1.36	1.35	1.30	C10-C11-C18	111.70	118.07	114.80
C21-C24	1.40	1.40	1.37	C10-C11-H31	107.41	90.26	106.60
C21-H25	1.09	1.10	0.93	C12-C11-C18	113.04	121.16	113.20
C23-C24	1.40	1.40	1.37	C12-C11-H31	109.60	89.67	106.60
C23-H26	1.09	1.10	0.93	C18-C11-H31	106.25	90.18	106.60
C24-H27	1.09	1.10	0.93	C11-C12-C13	121.45	120.45	122.90
N32-H33	1.01	1.00	0.86	C11-C12-C35	120.15	120.97	116.60
N32-H34	1.01	1.00	0.86	C13-C12-C35	118.27	118.58	120.40
C35-N36	1.17	1.15	1.14	C12-C13-O30	122.55	120.44	122.10
				C12-C13-N32	127.02	118.58	127.80
				O30-C13-N32	110.37	120.98	110.10
				C11-C18-C19	121.24	120.01	118.00
				C11-C18-C20	121.88	119.99	125.40
				C19-C18-C20	116.88	119.99	116.60
				C18-C19-C21	121.38	120.01	121.60
				C18-C19-H22	118.59	120.01	119.20
				C21-C19-H22	120.03	119.98	119.20
				C18-C20-C23	123.11	119.99	122.30
				C18-C20-F37	118.87	119.98	118.80
				C23-C20-F37	118.03	120.02	119.50
				C19-C21-C24	119.99	120.00	119.90
				C19-C21-H25	119.81	120.00	120.00
				C24-C21-H25	120.20	120.00	120.00
				C20-C23-C24	118.68	120.00	119.40
				C20-C23-H26	119.19	120.01	120.30
				C24-C23-H26	122.13	119.98	120.30
				C21-C24-C23	119.96	120.00	120.10
				C21-C24-H27	120.39	120.01	120.00
				C23-C24-H27	119.65	119.99	120.00
				C9-O30-C13	118.39	120.76	117.40
				C13-N32-H33	117.66	120.00	120.00
				C13-N32-H34	116.80	120.00	120.00
				H33-C32-H34	117.46	120.00	120.00

* Taken from Ref[15].

observed at 1033 cm^{-1}in the FT-Raman and reckoned at1035 cm^{-1} in DFT/B3LYP 6–311++G (d, p). Vibration wasreckoned experimentally and theoretically. The reckoned NH_2 scissoring vibration is magnificentin accord with documented.

4.2.2. C-F vibrations

The vibration inclusion of the bond betweenof carbon–fluorine atom is appraised to discuss heremerge of vibrations is feasible due to the diminution of the molecule symmetry and the existence of heavy atoms in the ambit of the molecule.Sundaraganesanet.al[21] assigned

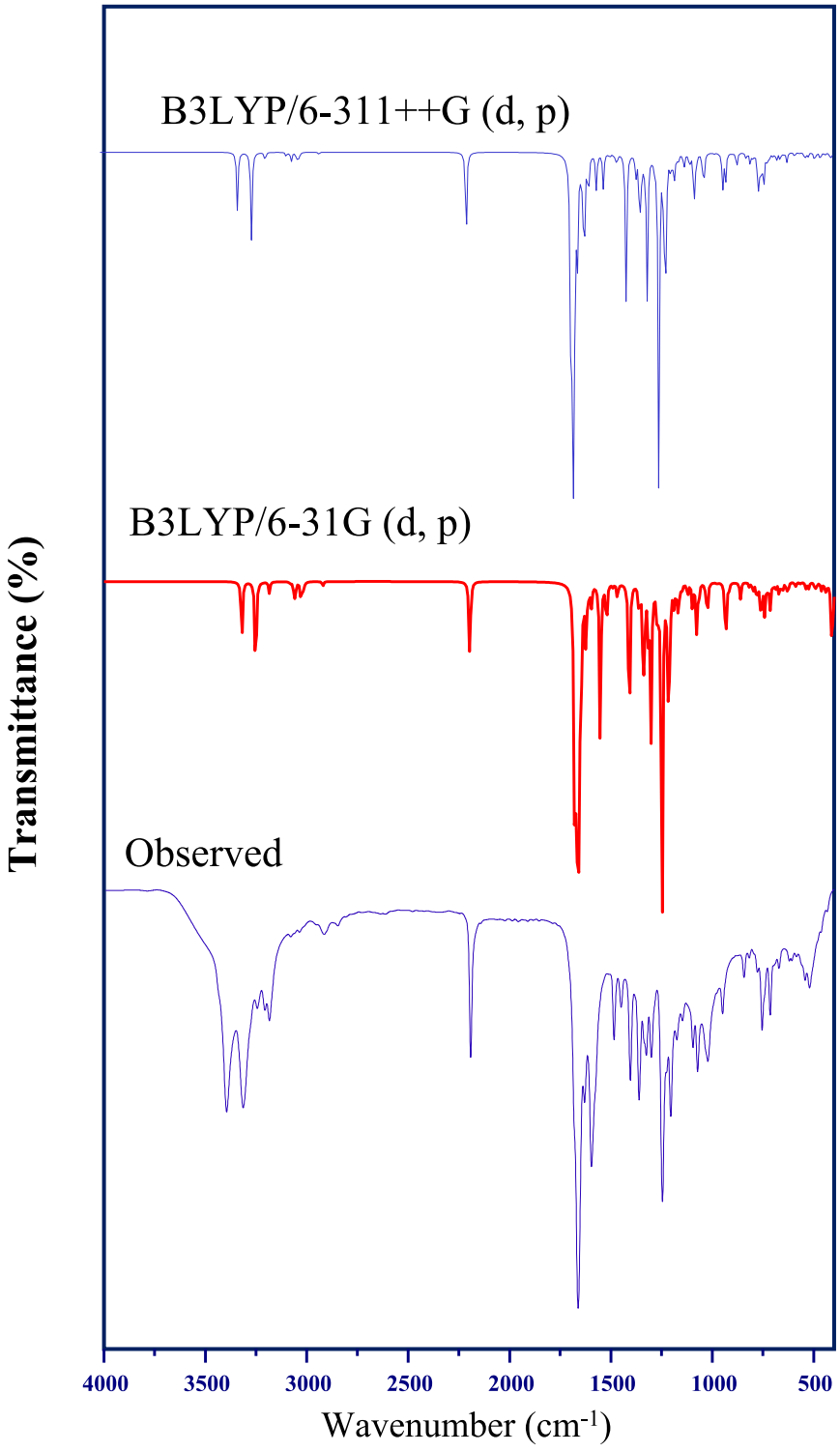

Fig. 2. FT-IR spectrum of AFBCC compound.

vibrations of the C-F group in the range of frequency1129 – 480 cm^{-1}. The FT-IR spectrum of AFBCC has sturdy bands at622 cm^{-1} and it encompasses 3 stretchings, one out-of-plane bending, and one in-plane bending vibration. C-F stretching vibration is observed at 1227 cm^{-1}. The vibration assignments ofin-plane bending were recorded at 627 cm^{-1}which has been reckoned by DFT/B3LYP/6–311++G (d, p). The reckoned C-F vibrations are in excellent accord with documented[22].

4.2.3. Carbonyl vibrations

The correlation of the C = O group with the amino group did not produce drastic and characteristic changes in the frequency. The nature of the carbonyl group actuates the oxygen as a lone pair of electrons. It enhances of carbonyl group due to the conjugation of hydrogen bonds. It escalates the conjugation, which enlargesthe intensity of Raman lines as well as the IR band intensities. The C = O vibrations take place in the range of 1850—1550 cm^{-1}, Nathiya et al[23]. The four C = O stretching vibrations are observed at 1680, 1671, 1662, 1649 cm^{-}1,and

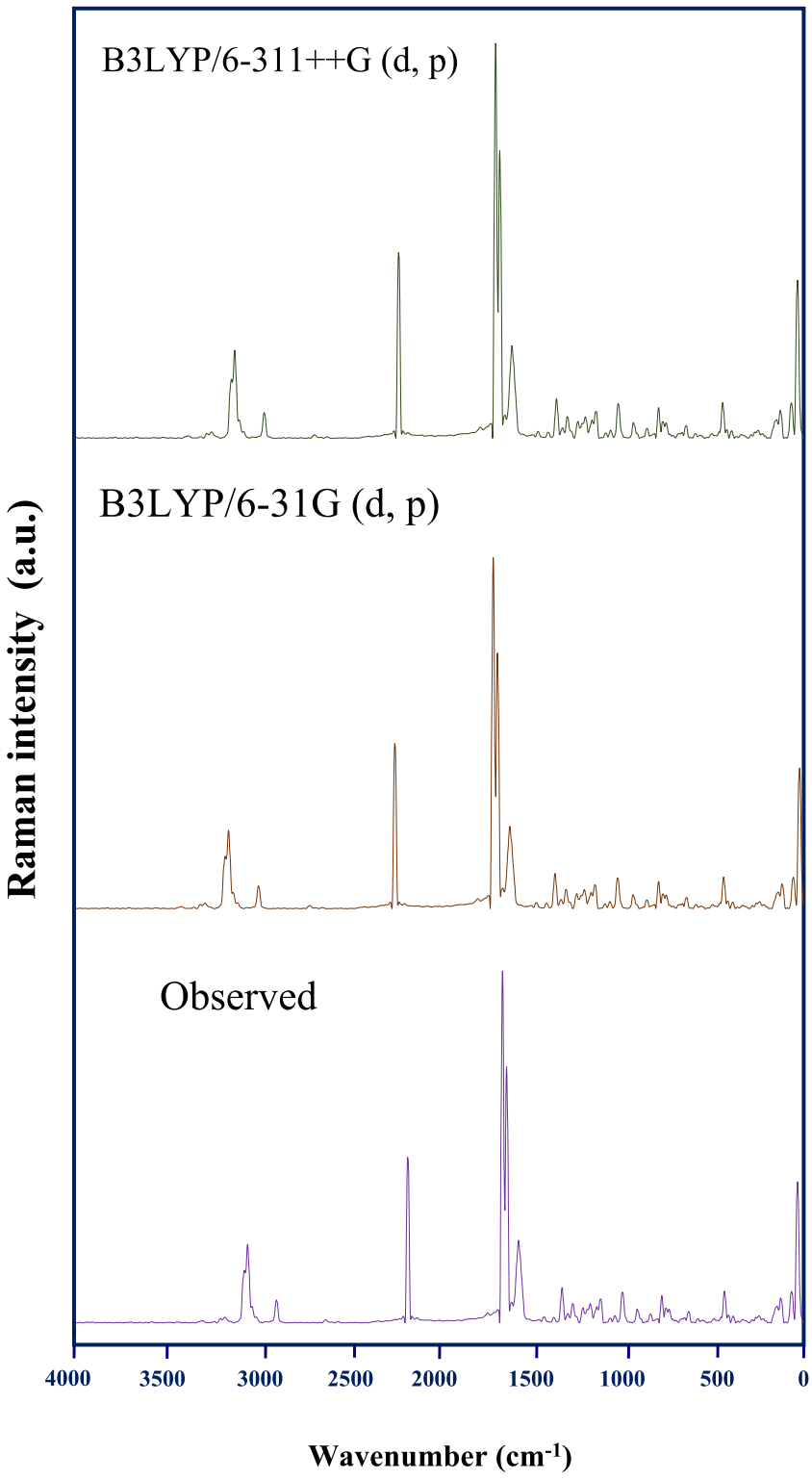

Fig. 3. FT-Raman spectrum of AFBCC compound.

1683, 1661 cm^{-1}in the FT-Raman spectrum. The FT-IR spectrum is reckoned at 1665 cm^{-1}in C = O stretching mode. The two in-plane bending modesare observed at 758,742 cm^{-1} and 785, 566,547 $cm^{-1}$are reckoned at out-of-plane bending vibrations in DFT/B3LYP 6–311++G (d, p).

4.2.4. Carbonitrile vibrations

The carbonitrile group is afflicted crucially as a new substituent of anthracene[19]. From AFBCC compound encompasses a carbonitrile group annexed to the anthracene ring has good intensity and has been absorbed in the range of 2200—1600 cm^{-1}. In the present work, theoretically, reckoned value υ(12) is allocated to the C≡N group stretching contributing 98 % of PED, and it is in accord agreement with our experimental spectrum observed as a strong apex in FT-Raman spectrum at 2197 $cm^{-1}$and the very strong apex in FT-IR spectrum at 2196 cm^{-1}, A Esme et al[24]. The carbonitrile stretching vibrations are reckoned in

Table 2
observed and calculated FT-IR and FT-Raman frequencies for 2-Amino-4-(3-hydroxyphenyl)-5,10-dioxo-5,10-dihydro-4*H*-benzo[*g*]chromene-3-carbonitrile.

S. No.	Observed wavenumbers (cm^{-1})		Calculated wavenumbers (cm^{-1})		Vibrational assignments (%PED)
			Scaled		
	FT-IR	FT-Raman	B3LYP/6-31G	B3LYP/ 6–311++G	
	3319		3325	3320	$\upsilon_{ass}NH_2$(99)
	3250		3256	3252	υ_{ss} NH_2(98)
	3190	3183	3189	3185	υCH(98)
		3083	3085	3082	υCH(98)
		3066	3068	3064	υCH(98)
	3057		3060	3057	υCH(98)
		3033	3034	3030	υCH(98)
			3026	3021	υCH(97)
	3014	3016	3019	3015	υCH(97)
			3007	3002	υCH(98)
	2919		2924	2920	υCH(98)
	2196	2197	2200	2196	υCN(98)
		1683	1685	1680	υCO(86), δCO(16)
			1676	1671	υCO(85), δCO(16)
	1665	1661	1670	1662	υCO(82), υCN(12)
			1654	1649	υCO(72), υCN(12), $\delta_{scis}NH_2$(10)
	1633	1633	1639	1635	υCC(82), δCH(14)
			1626	1623	υCC(80), δCH(15)
			1618	1611	$\delta_{scis}NH_2$(82)
	1599	1596	1599	1597	υCC(76), δCH(17)
			1560	1553	υCC(76), $\delta_{scis}NH_2$(12)
			1526	1522	δCH(78), υCF(10)
	1487		1494	1490	δCH(80)
		1466	1473	1468	δCH(80)
	1452		1460	1453	δCH(82)
	1407		1414	1410	υCN(79),υCO(16)
		1399	1347	1340	υCC(76),δCH(12)
	1364	1360	1366	1362	δCH(76),υCC(10)
	1328		1335	1330	υCC(74),δCH(16)
		1316	1321	1315	δCH(75)
	1303	1302	1310	1302	υCO(68), υCC(18), δCO(12)
			1290	1286	δCH(70)
			1275	1271	δCH(70)
	1248	1249	1253	1248	δCH(72), υCO(10)
			1232	1227	υCF(69),δCH(21)
			1221	1215	δCH(68), υCC(20)
	1207	1207	1212	1207	δCC(72), υCN(16)
			1194	1189	υCC(68), δCH(21)
	1177		1182	1178	δCH(70), υCF(12)
		1166	1175	1167	δCH(75)
			1163	1158	δCH(75)
	1149	1151	1157	1150	δCH(68)
			1129	1122	υCC(68)
	1097	1099	1102	1098	υCC(70)
	1074		1080	1077	υCC(70)
		1067	1069	1066	υCC(73)
		1033	1040	1035	$\Sigma_{rock}NH_2$(66)
	1024		1032	1025	γCH(67)
			1009	1003	γCH(68)
			981	977	γCH(66)
	951	949	956	950	γCH(66)
		933	939	934	γCH(68)
			925	918	γCH(68)
			908	904	γCH(68)
		883	892	885	υCC(65), δCN(10)
			870	862	υCC(65), υCC(16)
	820	819	824	818	υCO(72)
		799	804	800	γCH(70)
		783	792	785	γCO(67), γCO(12)
	779		786	780	υCC(70)
			766	763	υCO(71)
	756		760	758	δCO(65)
			746	742	δCO(64)
			735	730	υCC(74)
	716		718	715	υCC(74)

Table 2 (*continued*)

S. No.	Observed wavenumbers (cm^{-1})		Calculated wavenumbers (cm^{-1})		Vibrational assignments (%PED)
			Scaled		
	FT-IR	FT-Raman	B3LYP/6-31G	B3LYP/ 6–311++G	
		699	706	700	γCC(68), γCN(16)
			691	688	δ_{ring}(72)
	673	672	674	670	υCC(72)
			656	654	υCC(70)
		633	640	635	υCC(72)
	622		627	623	δCF(66)
	587	583	590	585	δCNN(76)
			566	562	γCO(66)
	543		547	543	γCO(60)
		533	538	535	δ_{ring}(61)
	521		525	520	δ_{ring}(60)
	487		493	489	γ_{ring}(49)
		479	485	481	δ_{ring}(56)
	458		463	460	γCF(51)
		450	460	455	δ_{ring}(54)
			445	441	γ_{ring}(50)
		433	439	435	δ_{ring}(58)
			410	409	γ_{ring}(50)
			385	281	δ_{ring}(60)
		366	370	265	δ_{ring}(62)
			354	350	γ_{ring}(51)
			339	335	γ_{ring}(51)
			320	317	δ_{ring}(60)
		299	306	301	$\gamma_{ring}NH_2$(65)
		283	284	282	δ_{ring}(58)
		266	264	266	δ_{ring}(61)
			250	247	Butterfly(50)
			225	222	Butterfly(48)
			192	190	γ_{ring}(48)
		174	178	175	γ_{ring}(55)
			158	157	γ_{ring}(58)
			135	136	δ_{ring}(60)
		116	120	116	δ_{ring}(60)
			105	103	υCCN(59), γ_{ring}(16)
		83	85	82	γ_{ring}(51)
			62	60	γ_{ring}(50)
			58	55	γ_{ring}(52)
			40	41	γ_{ring}(52)
			35	32	τCC(48)
			28	25	τCC(48)

υ- stretching, υ_{ss}-symmetric stretching, υ_{ass}- asymmetric stretching, δ- in-plane bending, γ-out-of-plane bending, τ-twisting, σ-rocking, ρ-scissoring, ω-wagging.

Table 3
Computed value of global molecular descriptors of AFBCC.

Parameters (eV)	B3LYP/ 6-31G (d, p) eV	B3LYP/6–311++G (d, p) eV
E_{HOMO}	−6.012	−6.439
E_{LUMO}	−3.255	−3.631
Energy gap ΔE	−2.757	−2.808
Ionization Potential (*IP*)	6.012	6.439
Electron Affinity (*EA*)	3.255	3.631
Electronegativity (χ)	4.634	5.035
Chemical Hardness (η)	1.378	1.404
Chemical Softness (σ)	0.725	0.712
Chemical Potential (μ)	−1.378	−1.404
Electrophilicity index (ω)	0.689	0.702

the range of 2196, 1410 cm^{-1} in B3LYP/ 6–311++G (d, p). The in-plane bending vibration is reckoned at 590 cm^{-1}along with FT- IR and FT-Raman observed at 587 and583 cm^{-1}. The reckoned carbinitrile vibrations are in good accord with the documented.

4.2.5. C–H vibrations

In the AFBCC compound the typical provinces of C–H stretching

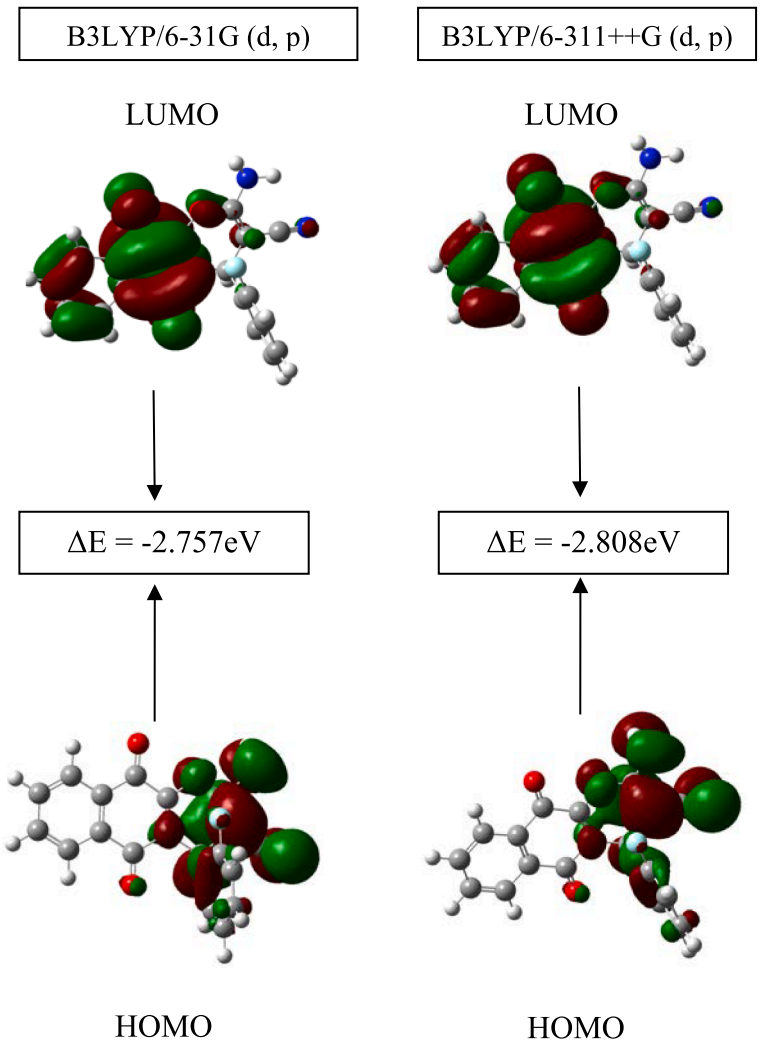

Fig. 4. Frontier molecular orbital of AFBCC compound.

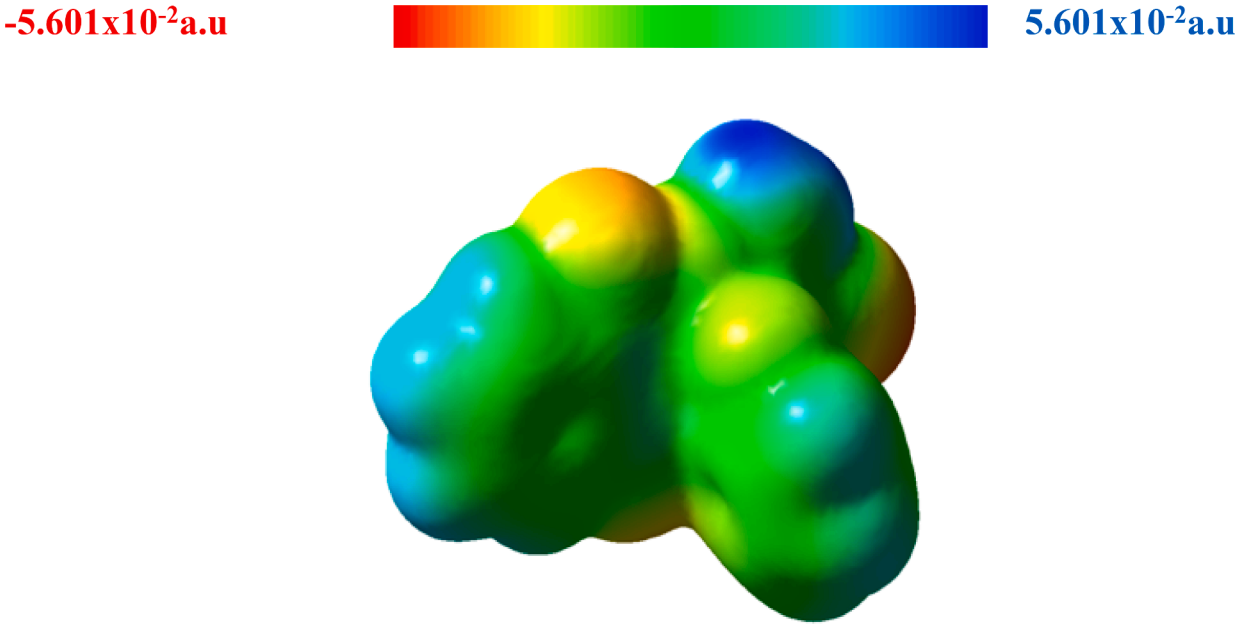

Fig. 5. Solid surface phase of AFBCC in Molecular electrostatic potential [MEP].

Table 4
Mulliken charges of AFBCC molecule.

Atom	B3LYP/6-31G (d, p)	B3LYP/6-311G ++ (d, p)
C1	−0.0890	−0.3047
C2	−0.0873	−0.0900
C3	0.0756	0.3303
C4	0.0749	0.7521
C5	−0.0927	−0.1108
C6	−0.0804	−0.3454
C7	0.2378	−0.5156
C8	0.2703	−0.6925
C9	0.2837	−0.5162
C10	0.1210	0.6378
C11	−0.1563	0.7495
C12	−0.0508	0.9587
C13	0.5582	0.0620
H14	0.1079	0.1876
H15	0.1365	0.2064
H16	0.1388	0.2090
H17	0.1100	0.1874
C18	0.0077	0.8927
C19	−0.0569	−0.0657
C20	0.3733	−0.5904
C21	−0.0928	−0.6871
H22	0.0904	0.1709
C23	−0.1374	−0.1343
C24	−0.0736	−0.1198
H25	0.0901	0.1774
H26	0.1005	0.2123
H27	0.0948	0.1750
O28	−0.5355	−0.2885
O29	−0.5264	−0.1075
O30	−0.5644	−0.1825
H31	0.2174	0.2845
N32	−0.6515	−0.4387
H33	0.3092	0.3237
H34	0.2969	0.3250
C35	0.2748	−1.3500
N36	−0.4851	−0.1343
F37	−0.2893	−0.1684

vibrations are in the regionof 3100 – 3000 cm^{-1}, Sivakumar et al[25]. In AFBCC compound comprised 38 vibrations which havesplitas 9 stretchings, 14in-plane bending, and 8 out-plane bending. The C–H stretchings are reckoned at 3187, 3082, 3064, 3057, 3030, 3021, 3015, and 3002 cm^{-1} theoretically and contributing 98 % of PED. According to, the prompt study, the FT-Raman bands are reckoned at 3183, 3083, 3066, 3033, 3016 $cm^{-1}$and FT-IR spectrum bands are reckoned at 3190, 3057, 3014 cm^{-1}. In the AFBCC compound, the in-plane bending vibrations occur1522, 1490, 1468, 1453, 1362, 1315, 1286, 1271, 1248, 1215, and 1150 cm^{-1}theoretically and out-of-plane bending vibrations are reckoned at 1025, 1003, 977, 950, 934, 918, 904, and 800 cm^{-1} theoretically. The out-of-plane bending and in-plane bending are contributing 70 %(υ58) and 82 %(υ25) PED[26].

4.2.6. C–C vibrations

The C–C stretching vibrations play apivotal role in the vibration analysis of aromatic compound and the spectrum appearing in the range of 1650–1400 cm^{-1} are reported by Amul et al[27]. The entitled compound encompasses24 vibrations which have splitinto 20 stretchings, 2 torsion in-plane bending, 1out-of-plane, and 1in-plane bending vibration. The C–C stretching vibrations (υ17) are reckoned theoretically and contribute82% of PED and the spectral bands are reported at 1635, 1623, 1597, and 1553 cm^{-1}.The spectrum bands 1633, and 1599 cm^{-1} have been recorded FT-IR experimentally. Concurrently, out-of-plane and in-plane bending vibrations are reckoned theoretically and contributing the PED (γ66) 68 %and (δ37) 72 %in the spectrum bands at1207 and 700 cm^{-1}. The spectrum bands 1633and 1596 cm^{-1} have been recorded FT-Raman experimentally. The reckoned C–C vibrations arein good accord with the documented.

4.2.7. Ring vibrations

The ring vibrational modes of the title molecule have been investigated depending on the vibrational spectra of recently distributed vibrations of the benzene ring is more useful in the distinguishing pieces of proof of the anthracene ring modes[28]. The out-of-plane and in-plane bending modes were reckoned at 178and 688 cm^{-1} in B3LYP/6-31G (d, p), and it contributed58%and 72 % of PED. The spectral bands are 538, 525, 485, 460, 439, 385 370, 320, 284, and 120 cm^{-1} in B3LYP/6–311++G (d, p) and the FT-IR spectrum bands are recorded experimentally in 521 cm^{-1} and the FT-Raman spectrum bands are also recorded at 533, 479, 450, 433, 366, 283,266, 116 cm^{-1}. The out-of-plane bending bands were theoretically obtained 493, 445, 410, 354,339, 192, 158, 85, 62, 58, and 40 cm^{-1}. Concurrently, FT-Raman and FT-IR were experimentally recorded at 174and 487 cm^{-1}.

4.3. Frontier molecular orbitals

The HOMO and LUMO are two contrasting and crucial molecular orbitals performed in the appraised energies of the AFBCC molecule. It takes a lead role in the endurance of strength and reactivity of the molecule. HOMO implies the capability to proffer an electron concurrently LUMO implies the capability to accept the electron. Inthe AFBCC compound occupied electrons always reside on orbitals with positive energies and the unoccupied electron has negative energy. By applying HOMO, LUMO orbital energies which can compute the ionization potential,electron affinity, chemical softness, chemical hardness, and electrophilicity index are labelled as Global reactivity descriptors[29].

It is a critical parameter in Global reactivity descriptors and the between the molecular orbitals labelled as energy gap (ΔE)

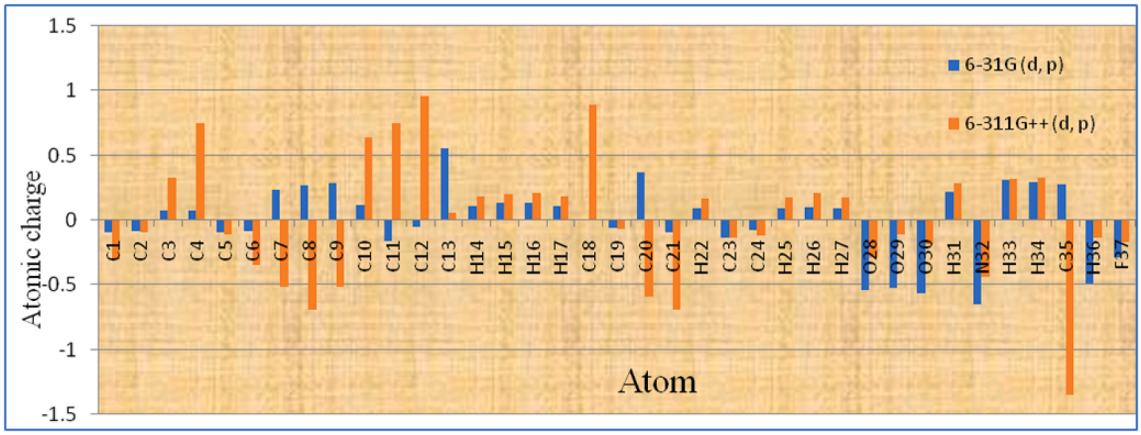

Fig. 6. Mulliken charge for AFBCC molecule.

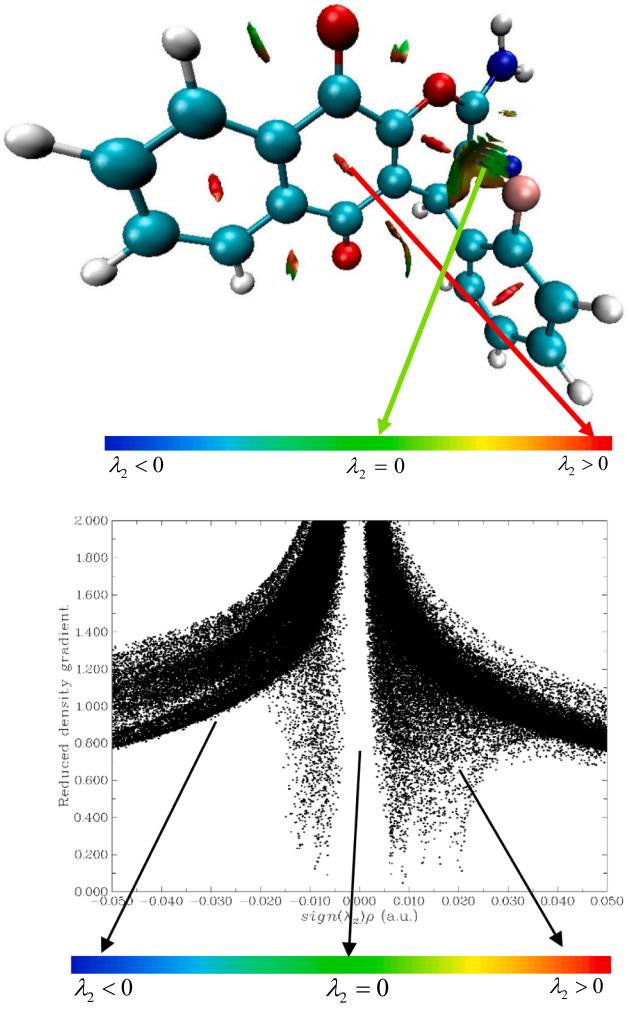

Fig. 7. RDG surface map and Scaling of weak interaction of AFBCC.

Table 5
Evaluation of drug-likeness prediction.

Descriptors	Calculated	Expected
Molecular mass	346.31	<500
Hydrogen bond acceptor	5	<10
Hydrogen bond donor	1	<5
Log P	2.09	<5
Molar refractivity	88.87	40–130

$$\Delta E = E_{HOMO} - E_{LUMO}$$

The theory of molecular orbital accesses the HOMO energy correlated to ionization potential by Koopman's theorem [28] and LUMO energy correlated to electron affinity

$$IP = -E_{HOMO}$$

$$EA = -E_{LUMO}$$

The mid value of HOMO and LUMO is correlated to Electronegativity (χ) elucidated by Mulliken [28]

$$\chi = \frac{IP + EA}{2}$$

To compute the hardness and softness of the compound will be able to determine by applying the HOMO and LUMO energies

$$\text{Hardness } \eta = \frac{IP - EA}{2}$$

$$\text{Softness } \sigma = \frac{1}{\eta}$$

The mid value of electron affinity and ionization potential is taken as a chemical potential and labelled as (μ)[30]

$$\mu = -\frac{IP + EA}{2}$$

From the results of chemical hardness (η) and chemical potential (μ) will be able to compute the electrophilicity index (ω)[30].

$$\omega = \frac{\mu^2}{2\eta}$$

The computed HOMO, LUMO, and energy gap in B3LYP/6311G++ (d, p) level are illustrated. From the conclusively, we take five contrasting pairs of the energy gap. The HOMO-LUMO = -2.808 eV, HOMO-1 -LUMO-1 = -5.330 eV, HOMO-2 -LUMO-2 = -5.934 eV, HOMO-3 -LUMO-3 = -6.956 eV, HOMO-4-LUMO-4 = -7.246 eV, HOMO-5-LUMO-5 = -7.447 eV. Using Koopman's hypothesis the ionization potential (IP = 6.439 eV) of the molecule system is equal to the negative of the orbital energy in the HOMO. The energy of the electron affinity (EA = 3.631 eV) is the neutral molecule and the radical anion[31].The other chemical properties are declared in Table 3 and vision in Fig. 4.

4.4. Molecular electrostatic potential (MEP)

TheMEP is correlated to the electron density and its very effective interpretation in understanding the sites of nucleophilic and electrophilic reactions. The electrophilic is a negative charge of electrons. The nucleophilic reactants have a positive chargeof electrons and it doesn't use in bonds[32]. The tendency to obtain electrons for a specific site pursues the regulations Red < Yellow < Green < Light blue < Blue. The blue region betokens positive, the red region betokens the negative electrostatic potential and the Green betokens the zero charge [33]. The pictorial of MEP mapped the [AFBCC] molecule that had computed in the basis set of 6–311++G(d, p) at the level of theory. The colour codes of the map that exposes in the range from $-5.601x10^{-2}$ a.u and $5.601x10^{-2}$ a.uwhich exhibit the strongest distribution of positive and negative charge of the [AFBCC] molecule and its pictorial is shown in Fig. 5. The N32, H33, and H34 atoms of the amino group cite in the positive region. The C35, N36, C8, C7, O28, and O29 atoms of the amino and carbonitrile group in the molecule cite in the negative region and other molecules have almost neutral electrostatic potential.

4.5. Mulliken population analysis

Mulliken charge plays an indispensable role in quantum chemical calculations to describe the potentiality of hydrogen bonding and the atomic charge values[34]. The principle of Mulliken charge, an exhaustive basis set for a molecule can be spanned by depositing a large set of functions on a single atom. Mulliken atomic charges are computed at B3LYP/6-31G (d, p) and B3LYP/6-311G++ (d, p) in a gas phase. It affords the appraising partial atomic charge carried out by the mode of computational chemistry. The atomic charges are vitally crucial for the molecular system because they affect the electronic structure, dipole moment, polarization, and chemical activity[35]. In the basis set 6-31G (d, p) the most immense appraisal is C13 = 0.5582 and the undermost appraisal is N32 = -0.6514 concurrently 6-311G++ (d, p) basis set the most immense and undermost appraisal are C12 = 0.958691 and C24 = -1.350007. The gross charges of AFBCC gained by Mulliken population inquiry with DFT/B3LYP/6-31G (d, p) and 6-311G++ (d, p) strategy are logged in Table 4, where the negative charges on C1, C2, C5-C9, C20-C24, O28-O30, N32, C35, N36, F37and positive charges on C3,C4,C10-

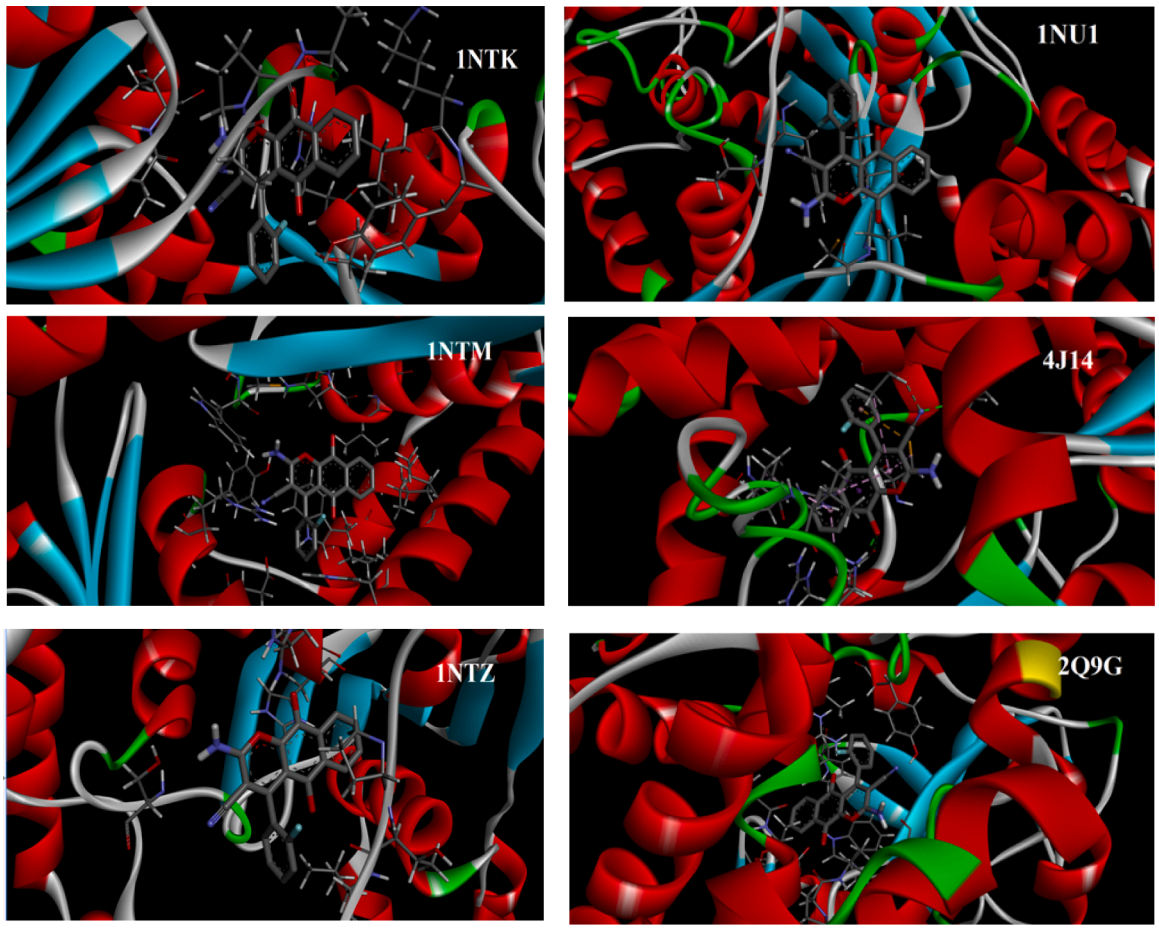

Fig. 8. Molecule docked into Antifungal [4 J14], Cytochrome [2Q9G],Ubiquinol- cytochrome-c reductase inhibitor [1NTK, 1NTM, 1NTZ, 1NU1] with AFBCC [ligand].

C13,H14-H17, C18, H22, H25-H27, H31, H33,H34. From the computed charges most of the hydrogen atoms are positive regions similarly the negative region represents the carbon atom because the title of the compound appertains to an amino group that encompasses fluorine and carbonitrile [36]. The graphical presentation is displayed in Fig. 6.

4.6. Non-covalent interaction

Reduced Density Gradient (RDG) is a rudimentary dimensionless quantity in DFT used to interpret the deflection from a homogenous electron distribution[37].Non-covalent interaction (NCI) is used tounderstand the weak interaction, strong repulsion, and strong attraction of the AFBCC compound using the Multiwfn3.8 software.From the RDG, at low densities is computed by using the formula

$$RDG(r) = \frac{1}{2(3\pi^2)} \frac{|\nabla\rho(r)|}{\rho(r)^{4/3}}$$

This interaction between the atoms of the AFBCC structure is determined by the small values of RDG. The blue indicateshydrogen bond, red indicates steric effect, green indicates Vander Waals interaction. Its properties as a bonding descriptor have been thoroughly highlighted by the NCI method. The RDG surface map has obtained the steric effect in the anthracene ring and the Vander Waals interaction is presented in the outer ring of the anthracene and is visualized in Fig. 7. In order to distinguish between repellent ($\lambda_2 > 0$ non-bonded) and attractive ($\lambda_2 < 0$ bonded) interactions, the λ_2 sign was adopted[38].

4.7. Prediction of biotic activity

The drug-likeness is the first step analysis of the biotic activity where the title compound is suitable or not. Using theprogram of the SwissADME"https://www.swissadme.ch/"analyze the physicochemical characteristics, drug-likenature, and pharmacokinetic qualities of the compound to aid drug discovery [39]. The AFBCC obeys the rule of Lipinski and it has zero violation. Simultaneously, the rule of Ghose, Egan, Muegge, and Veber was also obeyed. The percentage absorbance of the AFBCC molecule is 76.85 was reckoned by using the formula [40]

$$\%AB = 109 - 0.345TPSA$$

Finally, the physicochemical properties are proclaimed in Table 5 and the expected values are taken from the literature survey [41]. The molecular formula is C20H11N2O3, it has a bioavailability score of 0.56 and a Topological Polar Surface Area (TPSA) is 93.18 Å^2.

4.8. Molecular docking

The target of docking is to attain an optimized conformation and relative orientation between protein–ligand. Molecular docking is a computational technique that forecasts the binding site of protein and ligand. The significance of docking is intensely relevant in cellular docking and key to rational drug design. The properties of the ligand were diagnosedby PASS online software and it's helpful to forecast the biotic activity of the AFBCC compound as a ligand that correlates with protein[42]. Docking is the spotting of the low-energy binding modes of a ligand, enclosed by the active site of a receptor. Based on the disparate

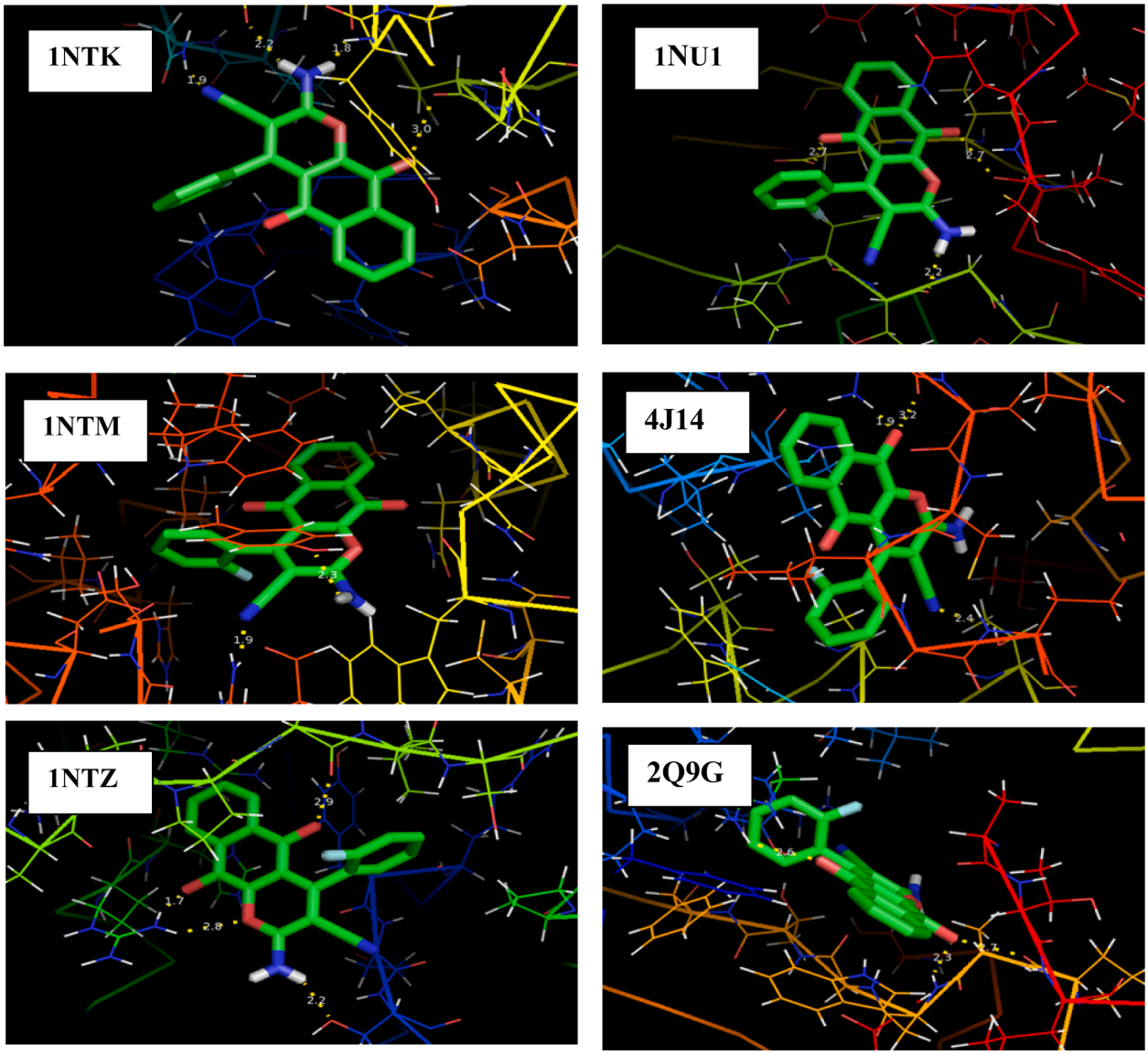

Fig. 9. Binding pose of the protein–ligand in the molecular docking.

properties were analyzed which accumulated the protein directly from the protein data bank (PDB) for the specified ligand[43]. The docking was effectuated by Auto Dock Tool (ADT) software and the 3-dimensional visual and 2-dimensional visual are clasping by Discovery Studio softwarewhile using Pymol software to clear away water molecules and co-crystallized ligand.ADT graphical user interface was used to compute the Kollman charge and the polar hydrogen[32].

4.8.1. Ubiquinol-cytochrome-c reductase inhibitor

Cytochrome is an integral membrane protein complex is important to photosynthesis and cellular respiration. The two inhibitors acquired separate portions of the Q(i) pocket and competed with the substrate for binding. The protein 1NTK isbinding with the ligand. The RMSD value of the protein–ligand is 49.583 Å and some amino acids (aspartate, tryptophan, asparagine, and proline) are present in the binding site of the ligand.The crystal structure of the 1NTMcomplex at 2.4 Å interacts with AFBCC to act as a ligand. The RMSD value of the protein–ligand is 151.354 Å and some acid of amino (arginine, tyrosine, glutamine, leucine) are presented in the binding site of the ligand. The crystal structure of 1NTZis complex bound with Ubiquinone and the crystal structure of 1NU1iscomplexed with 2-nonyl-4-hydroxyquinoline N-oxide interacts with ligand [AFBCC] and many amino acids (threonine, arginine, serine, cysteine, glutamic, phenylalanine) present in this binding site of protein–ligand[44]. The binding pose of the title molecule is shown in Figs. 8 and 9.

4.8.2. Antifungal

A medication known as an antifungal agent selectively removes fungal pathogens from a host with a low level of harm.Even the third-generation antifungal azoles, while having three generations, exhibit undesirable interactions with cytochrome P450 enzymes. Inthe current investigation,co-crystallized the P450 with posaconazole at 2.5 Å resolutions. The posaconazole-bound CYP46A1 crystal structure was compared to P450 crystal structures in complexes with other medicines, including the antifungal voriconazole and clotrimazole.The protein structure of4J14 interacts with ligand [AFBCC] and some amino groups are presented (threonine, lysine, arginine, alanine) in the binding site of the protein–ligand interaction. The bond distance of protein–ligand is 2.4, 1.9, 3.2, 2.8 Å the RMSD value is low while correlating with other proteins because the AFBCC is a soft molecule[45].

4.8.3. Cytochrome

Cytochrome P450 is entitled CYP. CYP enzymes have been recognized in all life kingdoms as well as viruses. Most of the drugs may

Table 6
Inhibition zone levels and binding energy of AFBCC molecular docking.

Ligand	Protein name	Protein ID	Bond distance (Å)	Amino acid	Binding energy (kcal/mol)	Inhibition constant	RMSD (Å)
2-Amino-4-(2-fluorophenyl)-5,10-dioxo-5,10-dihydro-4*H*-benzo[g]chromene-3-carbonitrile	Ubiquinol-cytochrome-c reductase inhibitor	1NTK	1.8	PRD	−7.23	5.02 μM	49.583
			2.2	ASP			
			1.9	ASN			
			3.0	TRP			
		1NTM	1.9	ARG	−7.43	3.59 μM	151.354
			2.3	TYR			
			2.8	GLN			
			3.4	LEV			
		1NTZ	2.9	THR	−8.62	476.57 nM	134.857
			1.7	ARG			
			2.8	ARG			
			2.2	SER			
		1NU1	2.7	CYS	−7.59	2.74 μM	154.938
			2.2	THR			
			2.7	GLU			
			1.8	PHE			
	Cytochrome	2Q9G	1.8	TYR	−9.03	241.64 nM	31.546
			2.6	ARG			
			2.7	PRO			
			2.3	TRP			
	Antifungal	4 J14	2.4	THR	−8.79	362.55 nM	30.206
			1.9	LYS			
			3.2	ARG			
			2.8	ALA			

reduce or raise the activity of varying CYP isozymes eitherby inducing the biosynthesis of an isozyme (enzyme induction)orby directly inhibiting the activity of the CYP enzyme inhibition. The term "P450″ is derived as the absorption wavelength of the spectrophotometric peak which iscomplexed with carbon monoxide andthe reduced state. The protein 2Q9G interacts with the specified ligand; an amino group such as (threonine, alanine, lysine, and arginine) is presented in the binding site of the proteinligand [46]. In CYP protein (2Q9G) binding energy is very low and it correlates with other proteins which have mentioned above as proclaimed in Table 6.

5. Conclusion

The structural characteristics of AFBCChave been recountedby spectroscopic and computational methods. The IR and Raman spectra of the molecule were recorded and discussed. Optimized structural parameters of the title compound were found to have good agreement with the experimentally measured bond length andbond angle.The intramolecular charge transfer occurs within the molecule due to the energy gap of the frontier molecular orbital, which enhanced the bioactivitiesspecifically the Ubiquinol-cytochrome-c reductase inhibitor, Antifungal, and Cytochrome activities of the molecule. Molecular docking studies show protein–ligand interactions employing H-bond.

Declaration of Competing Interest

The authors declare that they have no known competing financial interests or personal relationships that could have appeared to influence the work reported in this paper.

Data availability

The authors do not have permission to share data.

References

[1] A.K. Jordão, M.D. Vargas, A.C. Pinto, F.de.C. da Silva, V.F. Ferreira, Lawsone in organic synthesis, RSC Adv. 5 (2015) 67909–67943, https://doi.org/10.1039/C5RA12785H.
[2] Y.J. Kim, J.H. Kim, M.-S. Kang, M.J. Lee, J. Won, J.C. Lee, Y.S. Kang, Supramolecular electrolytes for use in highly efficient dye-sensitized solar cells, Adv. Mater. 16 (2004) 1753–1757, https://doi.org/10.1002/adma.200306664.
[3] C. P. Dell and C. W. Smith, Antiproliferative derivatives of 4H-naphtho[1,2-b] pyran and process for their preparation, Ref. Chem. Abstr. 119 (1993) 139102d. 119 (1993).
[4] J.M. Doshi, D. Tian, C. Xing, Structure−activity relationship studies of ethyl 2-amino-6-bromo-4-(1-cyano-2-ethoxy-2-oxoethyl)-4 H -chromene-3-carboxylate (HA 14–1), an antagonist for antiapoptotic Bcl-2 proteins to overcome drug resistance in cancer, J. Med. Chem. 49 (2006) 7731–7739, https://doi.org/10.1021/jm060968r.
[5] W. Kemnitzer, J. Drewe, S. Jiang, H. Zhang, J. Zhao, C. Crogan-Grundy, L. Xu, S. Lamothe, H. Gourdeau, R. Denis, B. Tseng, S. Kasibhatla, S.X. Cai, Discovery of 4-Aryl-4 H -chromenes as a new series of apoptosis inducers using a cell- and caspase-based high-throughput screening assay. 3. Structure−activity relationships of fused rings at the 7,8-positions, J. Med. Chem. 50 (2007) 2858–2864, https://doi.org/10.1021/jm070216c.
[6] R.R. Kumar, S. Perumal, P. Senthilkumar, P. Yogeeswari, D. Sriram, An atom efficient, solvent-free, green synthesis and antimycobacterial evaluation of 2-amino-6-methyl-4-aryl-8-[(E)-arylmethylidene]-5,6,7,8-tetrahydro-4H-pyrano [3,2-c]pyridine-3-carbonitriles, Bioorg. Med. Chem. Lett. 17 (2007) 6459–6462, https://doi.org/10.1016/j.bmcl.2007.09.095.
[7] M. Kidwai, S. Saxena, M.K. Rahman Khan, S.S. Thukral, Aqua mediated synthesis of substituted 2-amino-4H-chromenes and in vitro study as antibacterial agents, Bioorg. Med. Chem. Lett. 15 (2005) 4295–4298, https://doi.org/10.1016/j.bmcl.2005.06.041.
[8] A. Martínez-Grau, J. Marco, Friedländer reaction on 2-amino-3-cyano-4H-pyrans: Synthesis of derivatives of 4H-pyran [2,3-b] quinoline, new tacrine analogues, Bioorg. Med. Chem. Lett. 7 (1997) 3165–3170, https://doi.org/10.1016/S0960-894X(97)10165-2.
[9] R. Thomas, M. Hossain, Y.S. Mary, K.S. Resmi, S. Armaković, S.J. Armaković, A. K. Nanda, V.K. Ranjan, G. Vijayakumar, C. Van Alsenoy, Spectroscopic analysis and molecular docking of imidazole derivatives and investigation of its reactive properties by DFT and molecular dynamics simulations, J. Mol. Struct. 1158 (2018) 156–175, https://doi.org/10.1016/j.molstruc.2018.01.021.
[10] A. Shaabani, R. Ghadari, S. Ghasemi, M. Pedarpour, A.H. Rezayan, A. Sarvary, S. W. Ng, Novel one-pot three- and pseudo-five-component reactions: synthesis of functionalized benzo[g]- and dihydropyrano[2,3- g]chromene derivatives, J. Comb. Chem. 11 (2009) 956–959, https://doi.org/10.1021/cc900101w.
[11] W.Y.R.G. Parr, Density functional theory of atoms and molecules, Oxford University, New York, 1989.
[12] C. Lee, W. Yang, R.G. Parr, Development of the Colle-Salvetti correlation-energy formula into a functional of the electron density, Phys. Rev. B 37 (1988) 785–789, https://doi.org/10.1103/PhysRevB.37.785.
[13] A.D. Becke, Density-functional thermochemistry. III. The role of exact exchange, J. Chem. Phys. 98 (1993) 5648–5652, https://doi.org/10.1063/1.464913.
[14] G.W.T.H.B.S.G.E.S. M.J. Frish, Gaussian 09, Revision A.I, Gaussian, Inc., (2009).
[15] J. Zhang, X. Zhang, S. Yan, N. Ma, S. Tu, 2-Amino-4-(2-chlorophenyl)-5,10-dioxo-5,10-dihydro-4H-benzo[g] chromene-3-carbonitrile, Acta Crystallogr. Sect. E: Struct. Rep. Online 65 (2008), https://doi.org/10.1107/S1600536808039986.

[16] S. Abbas Manthri, R. Muhamed, R. Rajesh, V. Sathyanarayanamoorthi, Spectroscopic and quantum mechanical investigations of (2E)-3-(2H-1,3-benzodioxol-5-yl)-N-phenylprop-2-enamide using density functional theory method, 2018.
[17] S. Jeyavijayan, E. Gobinath, K. Viswanathan, J. Senthil Kumar, Vibrational spectroscopic investigations, DFT computations, nonlinear optical and other molecular properties of 3-bromo-5-fluorobenzonitrile, 2018.
[18] V. Balachandran, G. Mahalakshmi, A. Lakshmi, A. Janaki, DFT, FT-Raman, FT-IR, HOMO-LUMO and NBO studies of 4-Methylmorpholine, Spectrochim Acta A Mol BiomolSpectrosc. 97 (2012) 1101–1110, https://doi.org/10.1016/j.saa.2012.07.112.
[19] M. Hanif, E. Khan, M. Khalid, M.N. Tahir, S.F.de.A. Morais, A.A.C. Braga, 2-Amino-3-methylpyridinium, 2-amino-4-methylbenzothiazolium and 2-amino-5-chloropyridinium salts. Experimental and theoretical findings, J. Mol. Struct. 1222 (2020), https://doi.org/10.1016/j.molstruc.2020.128914.
[20] A. Atac, M. Karabacak, E. Kose, C. Karaca, Spectroscopic (NMR, UV, FT-IR and FT-Raman) analysis and theoretical investigation of nicotinamide N-oxide with density functional theory, Spectrochim Acta A Mol BiomolSpectrosc. 83 (2011) 250–258, https://doi.org/10.1016/j.saa.2011.08.027.
[21] N. Sundaraganesan, G. Elango, S. Sebastian, P. Subramani, Molecular structure, vibrational spectroscopic studies and analysis of 2-fluoro-5-methylbenzonitrile, 2009.
[22] K.S. and S.S. G.Raja, Analysis on vibrational spectra of Hexafluorobenzene based on density functional theory calculations, Elixir International Journal Computational Chemistry. 32 (2011) 2111–2115.
[23] A. Nathiya, H. Saleem, T. Jayakumar, A. Rajavel, N. Ramesh Babu, Molecular structure and vibrational analysis of 2-(4-methoxyphenyl)-2, 3-dihydro-1H-perimidine using density functional theory, Journal of New Developments Chemistry. 1 (2017) 70–99, https://doi.org/10.14302/issn.2377-2549.jndc-17-1488.
[24] A. Eşme, Quantum chemical calculations on the geometrical, conformational, spectroscopic (FTIR, FT-Raman) analysis and NLO activity of milrinone [5-cyano-2-methyl-(3,4'-bipyridin)-6(1h)-one] by using hartree-fock and density functional methods, 2017.
[25] C. Sivakumar, B. Revathi, V. Balachandran, B. Narayana, V.V. Salian, N. Shanmugapriya, K. Vanasundari, Molecular structure, spectroscopic, quantum chemical, topological, molecular docking and antimicrobial activity of 3-(4-Chlorophenyl)-5-[4-propan-2-yl) phenyl-4, 5-dihydro-1H-pyrazol-1-yl] (pyridin-4-yl) methanone, J. Mol. Struct. 1224 (2021), https://doi.org/10.1016/j.molstruc.2020.129286.
[26] T. Karthick, V. Balachandran, S. Perumal, A. Nataraj, Spectroscopic studies, HOMO-LUMO and NBO calculations on monomer and dimer conformer of 5-nitrosalicylic acid, J. Mol. Struct. 1005 (2011) 192–201, https://doi.org/10.1016/j.molstruc.2011.08.050.
[27] B. Amul, S. Muthu, M. Raja, S. Sevvanthi, Spectral, DFT and molecular docking investigations on Etodolac, J. Mol. Struct. 1195 (2019) 747–761, https://doi.org/10.1016/j.molstruc.2019.06.047.
[28] R. Sivakumar, S. Arivoli, M.K. Murali, K. Asini, DFT and Spectral Analysis of 5-Aziridinyl-3-hydroxymethyl-1-methylindole-4,7-dione, n.d. http://bulletinmonumental.com/.
[29] A. Viji, V. Balachandran, S. Babiyana, B. Narayana, V.V. Saliyan, Molecular docking and quantum chemical calculations of 4-methoxy-{2-[3-(4-chlorophenyl)-5-(4-(propane-2-yl) PHENYL)-4, 5-dihydro-1H-pyrazol-1-yl]- 1, 3-thiazol-4-yl} phenol, J. Mol. Struct. 1203 (2020), https://doi.org/10.1016/j.molstruc.2019.127452.
[30] C. Sivakumar, V. Balachandran, B. Narayana, V.V. Salian, B. Revathi, N. Shanmugapriya, K. Vanasundari, Molecular spectroscopic assembly of 3-(4-chlorophenyl)-5-[4-(propane-2-yl) phenyl] 4, 5-dihydro-1H pyrazole-1-carbothioamide, antimicrobial potential and molecular docking analysis, J. Mol. Struct. 1210 (2020), https://doi.org/10.1016/j.molstruc.2020.128005.
[31] A.T.A.K. Varsha Rani, Structural, spectroscopic, electronic, and nonlinear optical behavior investigations of π conjugated organic nonlinear optical chalcone derivative 3-(2,3- dichlorophenyl)-1-(pyridine-2-yl)prop-2-en-1-one using DFT, Indian J. Pure Appl. Phys. 59 (2012) 48–62.
[32] K. Vanasundari, V. Balachandran, M. Kavimani, B. Narayana, Spectroscopic investigation, vibrational assignments, Fukui functions, HOMO-LUMO, MEP and molecular docking evaluation of 4 – [(3, 4 – dichlorophenyl) amino] 2 – methylidene 4 – oxo butanoic acid by DFT method, J. Mol. Struct. 1147 (2017) 136–147, https://doi.org/10.1016/j.molstruc.2017.06.096.
[33] N. Afza, P. Devi, A. Kumar Verma, S. Shukla, H. Parveen, R. Kumar, S. Rai, A. Bishnoi, Synthesis, Spectroscopic & DFT studies of Novel N-((1H-benzo[d] imidazol-1-yl) methyl)-N-(2-(trifluoromethyl)phenyl)-4,5-dihydrothiazol-2-amine, 2021.
[34] S. Dheivamalar, B. Banu, The adsorption mechanism, structural and electronic properties of pyrrole adsorbed ZnO nano clusters in the field photovoltaic cells by density functional theory, 2019.
[35] A. Viji, B. Revathi, V. Balachandran, S. Babiyana, B. Narayana, V.V. Salian, Analysis of spectroscopic, quantum chemical calculations, molecular docking, RDG, ELF, anticancer and antimicrobial activity studies on bioactive molecule 2-[3-(4-Chlorophenyl)-5-(4-(propane-2-yl) phenyl-4,5-dihydro-1H-pyrazol-1-yl]-4-(4-methoxyphenyl)-1,3-thiazol, Chem. Data Collect. 30 (2020), https://doi.org/10.1016/j.cdc.2020.100585.
[36] S. Jeyavijayan, M. Ramuthai, P. Murugan, Investigating potential Part of α-Santonin in the treatment of SARS-CoV-2 and cervical cancer based on molecular docking strategy, Asian J. Chem. 33 (2021) 2313–2320, https://doi.org/10.14233/ajchem.2021.23308.
[37] R.A. Boto, J.-P. Piquemal, J. Contreras-García, Revealing strong interactions with the reduced density gradient: a benchmark for covalent, ionic and charge-shift bonds, Theor. Chem. Acc. 136 (2017) 139, https://doi.org/10.1007/s00214-017-2169-9.
[38] M. Kavimani, V. Balachandran, B. Narayana, K. Vanasundari, B. Revathi, Topological analysis (BCP) of vibrational spectroscopic studies, docking, RDG, DSSC, Fukui functions and chemical reactivity of 2-methylphenylacetic acid, Spectrochim Acta A Mol BiomolSpectrosc. 190 (2018) 47–60, https://doi.org/10.1016/j.saa.2017.09.005.
[39] S.V.D. Nisha, I.H. Joe, Molecular structure and spectroscopic exploration of antiviral drug docosanol: A combined experimental and DFT study, Braz. J. Phys. 52 (2022) 166, https://doi.org/10.1007/s13538-022-01168-7.
[40] K. Asgaonkar, S. Tanksali, K. Abhang, A. Sagar, Development of optimized pyrimido-thiazole scaffold derivatives as anticancer and multitargeting tyrosine kinase inhibitors using computational studies, J. Indian Chem. Soc. 100 (2023), 100803, https://doi.org/10.1016/j.jics.2022.100803.
[41] J.D.D. Tarika, X.D.D. Dexlin, S. Madhankumar, D.D. Jayanthi, T.J. Beaula, Tuning the computational evaluation of spectroscopic, ELF, LOL, NCI analysis and molecular docking of novel anti COVID-19 molecule 4-dimethylamino pyridinium 3, 5-dichlorosalicylate, Spectrochim Acta A Mol BiomolSpectrosc. 259 (2021), 119907, https://doi.org/10.1016/j.saa.2021.119907.
[42] A. Viji, V. Balachandran, S. Babiyana, B. Narayana, V.V. Salian, FT-IR and FT-Raman investigation, quantum chemical studies, molecular docking study and antimicrobial activity studies on novel bioactive drug of 1-(2,4-Dichlorobenzyl)-3-[2-(3-(4-chlorophenyl)-5-(4-(propan-2-yl)phenyl-4,5-dihydro-1H-pyrazol-1-yl]-4-oxo-4,5-dihydro-1,3-thiazol-5(4H)-ylidence]-2,3-dihydro-1H-indol-2-one, J. Mol. Struct. 1215 (2020), 128244, https://doi.org/10.1016/j.molstruc.2020.128244.
[43] N. Shanmugapriya, V. Balachandran, B. Revathi, B. Narayana, V.V. Salian, K. Vanasundari, C. Sivakumar, Quantum chemical calculation, performance of selective antimicrobial activity using molecular docking analysis, RDG and experimental (FT-IR, FT-Raman) investigation of 4-[{2-[3-(4-chlorophenyl)-5-(4-propan-2-yl) phenyl)-4, 5-dihydro- 1H- pyrazol-1-yl]-4-oxo-1, 3- thiazol-5(4H)-ylidene} methyl] benzonitrile, Heliyon. 7 (2021) e07634.
[44] X. Gao, X. Wen, L. Esser, B. Quinn, L. Yu, C.A. Yu, D. Xia, Structural basis for the quinone reduction in the bc1 complex: A comparative analysis of crystal structures of mitochondrial cytochrome bc1 with bound substrate and inhibitors at the Qi site, Biochemistry 42 (2003) 9067–9080, https://doi.org/10.1021/bi0341814.
[45] N. Mast, W. Zheng, C.D. Stout, I.A. Pikuleva, Antifungal azoles: Structural insights into undesired tight binding to cholesterol-metabolizing CYP46A1, Mol. Pharmacol. 84 (2013) 86–94, https://doi.org/10.1124/mol.113.085902.
[46] N. Mast, M.A. White, I. Bjorkhem, E.F. Johnson, C.D. Stout, I.A. Pikuleva, Crystal structures of substrate-bound and substrate-free cytochrome P450 46A1, the principal cholesterol hydroxylase in the brain, Proc. Natl. Acad. Sci. 105 (2008) 9546–9551, https://doi.org/10.1073/pnas.0803717105.

N. Thirughanasambantham was born in Tamil Nadu, India. He obtained B.Sc in Physics from St. Joseph's College, Trichy, Tamil Nadu in 2017 and M.Sc in Physics degree from Thanthai Hans Roever College (Autonomous), Peramabalur, Tamil Nadu in 2020. Since 2021, he pursing his Ph.D., Degree in Full-Time under the guidance of Dr. V. Balachandran, Associate Professor, Department of Physics, Arignar Anna Government Arts College, Musiri (Affiliated to Bharathidasan University), Tamil Nadu.

Dr. V. Balachandran was born in Tiruchirappalli, India. He obtained his B.Sc, M.Sc., and Ph.D degrees in Physics from the Bharathidasan University in the year 1987, 1990 and 2006, respectively. He worked as a Lecturer in Physics at Thanthai Hans Roever College, Perambalur from 1994 to 2007. Then he joined as Assistant Professor at Arignar Anna Government Arts College, Musiri. From 2020, he promoted as Associate Professor of Physics in the same institution. He published more than 200 research articles in various National and International Journals. His Scopus H-Index is 30, citations are 2879 and i-10 index is 85.

Dr. B Narayana was born in Kerala, India. He obtained his B.Sc and M.Sc degrees in Chemistry from the University of Calicut in 1981 and 1983 respectively. Later he obtained PhD in Chemistry from Mangalore University in the year 1990. He worked as a Faculty member at Mangalore University since 1988. He is superannuated from Mangalore University and will be joining as Vice Chancellor of K.K. University, Patna, Bihar. He is cited as Top 2% Scientists in the world –Stanford University, for the last 3 consecutive years-2020, 2021 and 2022. His Scopus H-Index is 37 and i-10 index is 244.

Dr. C. Sivakumar was born in Tamilnadu, India. He obtained his B.Sc Physics from Arignar Anna Govt Arts College, Musiri, Tamilnadu in 2007 and M.Sc and M.Phil in Physics from St. Joseph's College, Trichy, Tamilnadu in 2009 and 2011, He completed his P.hD at Bharathidasan University under the Guidance of Dr.V. Balachandran, Associate Professor, Department of Physics, Arignar Anna Govt Arts College, Musiri, Tamilnadu. From 2015 to till now, he is working as a Guest Lecturer in Department of Physics at Arignar Anna Govt Arts College, Musiri, Tamilnadu.

Dr. Jayashree Avvadukkam was born in Kerala, India. She obtained her B.Sc in Chemistry from Govt College Kasaragod, Kerala in 2011 and her M.Sc in Chemistry, securing the 2nd Rank, from Mangalore University, Karnataka in 2013. In the same year, she cleared the UGC-JRF examination, followed by the GATE in 2014. In 2021, she completed her Ph.D. at Mangalore University, working under the guidance of Prof. B. Narayana. From 2021 to 2022, she served as an Assistant Professor in the Department of Chemistry at Dr. Ambedkar Arts and Science College, Periye Kasaragod, and from 2022 to 2023 as a Guest Lecturer at the Department of Industrial Chemistry at Mangalore University.

Dr. M. Kavimani was born in Tamil Nadu, India. She obtained her B.Sc. in Physics from Chidambaram Pillai College for Women, Mannachanallur and her M.Sc. in Physics from Srimati Indira Gandhi College, Trichy, securing the 8th Rank, from Bharathidasan University, Tamil Nadu in 2012. She cleared the CSIR UGC-NET examination in 2012 and her M.Phil. in Physics from National College, Trichy securing 1st Rank. In 2019, she completed her Ph.D. in Arignar Anna Government Arts College, Musiri affiliated to Bharathidasan University, under the guidance of Prof. Dr. V. Balachandran. Since 2018 to till, she working as an Assistant Professor in the PG & Research Department of Physics, Cauvery College for Women (A), Trichy. She got the Young Scientist Fellowship by TNSCST in 2023 and got Summer Faculty Research Fellowship by IIT Delhi in 2023.